

# The dynamical evolution of Taurus–Auriga-type aggregates

Pavel Kroupa<sup>1,2</sup>, Jerome Bouvier<sup>1</sup>

<sup>1</sup>*Laboratoire d’Astrophysique de l’Observatoire de Grenoble, BP 53, F-38041 Grenoble Cedex 9, France*

<sup>2</sup>*Institut für Theoretische Physik und Astrophysik der Universität Kiel, D-24098 Kiel, Germany*

13 November 2018

## ABSTRACT

Star formation in the Taurus–Auriga (TA) molecular clouds is producing binary-rich aggregates containing at most a few dozen systems within a region spanning one pc without massive stars. This environment is very different to another well-studied star-forming event which produced the Orion Nebula cluster (ONC). The ONC contains a few thousand systems within a region of one pc including massive stars. Differences between these two environments have been found. Notably, the ONC has a significantly smaller binary proportion but a significantly larger number of isolated brown dwarfs (BDs) per star than TA. The aim of the present project is to investigate if these differences can be explained through stellar-dynamical evolution alone. The stellar-dynamical issue is very relevant because dense environments destroy binaries liberating BD companions, possibly leading to the observed difference between the TA and ONC populations. Here a series of high-precision  $N$ –body models of TA-like embedded aggregates are presented, assuming the standard reference star-formation model for the input populations according to which stars and BDs form with the same kinematical, spatial and binary properties. After a discussion of the general evolution of the aggregates, it is shown that the binary population indeed remains mostly unevolved. Therefore, TA-type star formation cannot have added significantly to the Galactic-field population. The standard model leads to BDs tracing the stellar distribution, apart from a high-velocity tail ( $v \gtrsim 1$  km/s) which leads to a more widely distributed spatial distribution of single BDs. The slow-moving BDs, however, retain a high binary proportion, this being an important observational diagnostic for testing against the embryo-ejection hypothesis. Inferences about the IMF and the binary-star orbital distribution functions are made in two accompanying papers with useful implications for star formation and the possible origin of BDs.

**Key words:** stars: formation – stars: low-mass, brown dwarfs – binaries: general – open clusters and associations: general – Galaxy: stellar content – stellar dynamics

## 1 INTRODUCTION

Stars appear never to form in true isolation, but mostly with partners which are typically clustered into groups. These contain from a few dozen stars, such as the aggregates in the TA star formation complex (Gomez et al. 1993; Briceno et al. 2002; Hartmann 2002), through to thousands of stars in rich clusters, such as the ONC (Hillenbrand & Hartmann 1998; Muench et al. 2002) to hundreds of thousands of stars in very rich and massive young globular cluster-type assemblages. By comparing the properties of stellar populations in such different environments we learn how different physical conditions determine the star-formation products. Owing to their proximity and similar age (about 1 Myr) the stellar groups in TA and the ONC are prime candidates for detailed inter-comparisons.

Observational campaigns have established that most stars in TA are in binary systems, while in the ONC the binary properties of low-mass stars appear to be similar to those of the Galactic-field population (Duchêne 1999). Stars more massive than about  $2 M_{\odot}$  have not formed in TA, while the ONC contains a number of O stars. The ONC has also been shown to contain many brown dwarfs (BDs) (Hillenbrand & Carpenter 2000; Muench et al. 2002), while there is a deficit of substellar objects in TA (Briceno et al. 2002). Furthermore, the stellar rotation distributions in the two star-forming regions are intrinsically different (Clarke & Bouvier 2000). The two physically different systems thus appear to produce different stellar

populations. However, closer inspection may indicate otherwise. Thus, massive stars cannot form in TA because the cloud cores are not massive enough. This does not necessarily imply that the stellar initial mass function (IMF) has a different form. It merely means that the most massive stars can only form if sufficient material is available. The higher frequency of binary stars in TA may be due to the TA aggregates being dynamically unevolved, given that the crossing time through an aggregate is about equal to the age of the stars or longer, while a typical star has crossed the ONC several times within its life-time. This would have reduced a TA binary frequency to the observed ONC level (Kroupa, Aarseth & Hurley 2001, hereinafter KAH), thus eroding the argument for different initial period distributions. Similarly, close encounters may have removed disk-breaking in the ONC leading to faster rotators, or there is a systematic difference in the observed stellar mass ranges in the two samples together with a mass-rotation dependence (Clarke & Bouvier 2000).

The recent affirmation by Briceno et al. (2002) that TA contains significantly fewer BDs per star than the ONC is an important clue that may indeed constitute the first direct evidence for a variation of the IMF, at least in the sub-stellar regime. The problem we are faced with in view of this empirical evidence, which implies a variation of a factor of two or so in the number of BDs per star, is that the surplus BDs detected in the ONC may be low-mass companions that have left their primaries due to encounters. This possibility, if confirmed, would again spoil the claim for a different sub-stellar IMF in TA.

To address this particular problem a number of stellar-dynamical models of embedded TA-like aggregates are calculated using the same methodology and assumptions as in a previous recent detailed study of the dynamical evolution of the ONC and the Pleiades cluster. This study by KAH finds rather excellent agreement with all available observational constraints (radial density profile, kinematics, IMF and binary properties for the ONC and the Pleiades) under a set of assumptions that define the outcome of star formation. These assumptions, which we refer to as the *standard reference star-formation model* (or just “standard model”), have previously been found to lead to an excellent agreement with the Galactic field population if the majority of stars form in small embedded clusters containing not more than a few hundred binaries (Kroupa 1995, hereinafter K2).

The calculations are performed with the Aarseth-NBODY6 variant GASEx described by KAH in their study of cluster formation. GASEx is a direct, high-precision  $N$ -body integrator which allows accurate treatment of close encounters and multiple stellar systems in clusters through special mathematical transformation techniques of the equations of motion (regularisation). Force-softening is not implemented. It is identical to Aarseth’s NBODY6 code apart from having additional input and output features and an additional routine for setting-up a realistic initial binary-star population. GASEx also allows the inclusion of a time-varying analytic background potential to model gas expulsion from an embedded cluster, and incorporates a local Galactic-tidal field into the equations of motion of each star. A comparison of the effect of gas-expulsion on an embedded cluster using hydrodynamical computations and  $N$ -body calculations assuming time-varying analytic background potentials leads to the same results (Geyer & Burkert 2001).

The purpose of this paper is to introduce the models and describe the evolution of TA-like aggregates thereby focusing attention on their BD members. Companion papers (Kroupa et al. 2003; Kroupa & Bouvier 2003) address, respectively, the (related) issues of IMF variation and binary systems in TA, and the implications this has for the origin of BDs and free-floating planetary mass objects. This paper begins with a description of the standard model (§ 2). The TA-like models studied here are introduced in § 3, and their evolution is described in § 4. The evolution of the binary systems is studied in § 5, and § 6 discusses how the relative distribution of the BDs and stars can be used to differentiate between formation models of BDs. The conclusions follow in § 7.

## 2 THE STANDARD REFERENCE STAR-FORMATION MODEL

A brief description of the standard model is presented here. It is useful as standardised and realistic initial conditions for  $N$ -body computations of star clusters. The standard model is defined by a minimal set of assumptions based on empirical and theoretical evidence that describe the outcome of star formation. The model has been developed in K2 to find the dominant star-formation events that produced the Galactic field population, taking as an initial boundary condition the observed pre-main sequence binary-star properties in TA. It accounts for the properties of short-period binary systems, but does not incorporate BDs. In the strict form, it therefore only applies to late-type stars with masses in the approximate range  $0.08 - 1 M_{\odot}$ . This model leads to stellar populations in good agreement with available observational data for Galactic-field main-sequence stars and pre-main sequence stars in dense clusters including the Pleiades (K2; Kroupa, Petr & McCaughrean 1999; KAH).

The standard model can be used to search for variations of the IMF or binary-star properties in dependence of star-formation conditions. If a population is found which has an abnormal IMF or unusual binary-star properties, and if dynamical and stellar evolution cannot reproduce these observations given the standard model, then a very strong case for a variation of the IMF or binary-star properties will have been found. An example of such an application is provided by Kroupa (2001). Thus, if a modelled population is found to deviate significantly from an observed population, then this would imply that the

initial conditions for that population deviate from the standard model and thus that there is a variation of the star-formation products since the standard model can reproduce a number of populations with very different ages.

We note that while the available results and notably the visualisation of pure hydrodynamical collapse computations are spectacular (Bate 2003), it is not attempted to use these results as input for the  $N$ -body calculations. Feedback from the forming stars via outflows and radiation will probably significantly change the outcome of the numerical hydrodynamical experiments. These allow most of the gas to accrete, while in reality star-formation reaches an efficiency of less than 40 per cent (Lada 1999; Matzner & McKee 2000). In particular, it is noted that the modern collapse computations that lack feedback and radiative energy transport as well as magnetic forces lead to important lessons about the gravitational processes acting during the onset of star formation, but they are likely to form groups of “stars” that are too compact and therewith too dynamically violent. Stellar feedback is also likely to trigger the formation of other stars nearby, which again is not captured by the existing cloud collapse computations. It is not clear how feedback can be included in a self-consistent manner in such collapse computations, unless some parametrisation for example of the collimated outflows is attempted, and because full radiation transfer poses prohibitive challenges on the computational requirements. It is for this reason that the  $N$ -body approach to young embedded clusters will remain a major work-horse in the future.

The philosophy followed here is to approach the outcome of star formation from the “other side” by studying how well-defined physical processes (mostly stellar-dynamics) affect binary-star properties and stellar distributions. Our ansatz with an analytical time-varying potential (§ 3) assumes the newly formed stars to have decoupled hydrodynamically from their gaseous environment and captures the most important physical aspect of the problem, namely the initial confinement of the stellar population in their embedded cluster (Geyer & Burkert 2001). By this approach we infer the properties the stellar distribution functions should have at the point in time when the dynamics becomes dominated by point-mass gravitational interactions, and which should ultimately come out of the cloud-collapse plus feedback work that will hopefully become available in the (distant) future.

The standard model assumes

- (i) All stars are paired randomly from the IMF to form binary systems with primary mass  $m_p$  and companion or secondary mass  $m_s \leq m_p$ .
- (ii) The distribution of orbital elements (period, eccentricity and mass ratio) does not depend on the mass of the primary star, but allowance for eigenevolution (see below) is made.
- (iii) Stellar masses are not correlated with the phase-space variables (no initial mass segregation in a cluster).

Assumption (i) leads to a flat initial mass-ratio distribution for late-type primaries,  $f_q$ , (fig. 12 in K2; fig. 5 in Malkov & Zinnecker 2001), and is consistent with the flat mass-ratio distribution for  $q \equiv m_2/m_1 \gtrsim 0.2$  derived from observational data of pre-main sequence binaries by Woitas, Leinert & Köhler (2001). They state that “these findings are in line with the assumption that for most multiple systems in T associations the components’ masses are principally determined by fragmentation during formation and not by the following accretion processes”. This in turn is supported by the finding that the mass function of pre-stellar cores in  $\rho$  Oph already has the same shape as the Galactic-field IMF thus indicating that the fragmentation of a molecular cloud core defines the distribution of stellar masses (Motte, André & Néri 1998; Bontemps et al. 2001; Matzner & McKee 2000). The above assumptions include implicitly that any initial multiple proto-stellar systems have decayed within a few crossing times (typically  $10^4$  yr, Reipurth 2000) to form the binary-rich initial population seen in the about 1 Myr old populations studied here.

By extending the standard model to include BDs we change the stellar pairing properties by allowing stars to have BD companions. The fraction of such systems may be appreciable but depends on the IMF for BDs. It is the purpose of the present study to investigate the consequences of the extension. Likewise, extension of the standard model to massive stars implies that most O stars will have low-mass companions, but here we are not concerned with massive stars.

Assumption (ii) is posed given the indistinguishable period distribution function of Galactic-field G-dwarf, K-dwarf and M-dwarf binary systems (fig. 7 in K2). The discordant period distributions between the pre-main sequence binaries and the Galactic-field systems can be nicely explained by disruption of wide-period binaries in small embedded clusters containing a few hundred stars. This destruction process also leads to the observed mass-ratio distribution for G-dwarf primaries in the Galactic field. The model is also in good agreement with the observed smaller binary fraction of M dwarfs than of K dwarfs and G dwarfs (K2).

Assumption (iii) allows investigation of the important issue whether massive stars need to form at the centres of their embedded clusters to explain the observed mass segregation in very young clusters such as the ONC (Hillenbrand 1997; Muench et al. 2003). Assumption (iii) is motivated by observations which indicate that at least some massive stars appear to be surrounded by massive disks suggesting growth of the massive star by disk accretion rather than through coagulation of proto-stars (Figueredo et al. 2002; Cesaroni et al. 2003), and by the observations that forming embedded clusters are typically heavily sub-clustered, with massive stars forming at various locations (e.g. Motte, Schilke & Lis 2002). Cesaroni et al. (2003) find the massive proto-stars in the forming cluster G24.78+0.08 to lie at various locations within the central region with a radius of 0.5 pc, a region that also appears to be heavily sub-structured. On-going  $N$ -body work is addressing the issue if

dynamical mass-segregation can account for the observed mass segregation in the ONC for example, in which sub-structure has been erased already (Scally & Clarke 2002). Available state-of-the art work by Bonnell & Davies (1998) suggests that in the absence of initial subclustering two-body relaxation may not be able to account for the observed mass segregation. This work is based on Aarseth's NBODY2 code which requires force softening to treat close stellar encounters, and more recent attempts with GASEX indicates that two-body relaxation may lead to the observed mass segregation if the initial configuration of the binary-rich cluster is very compact (Kroupa 2002). This topic needs to be studied in more detail. The alternative scenario is that coagulation of forming proto-stars in the densest embedded cluster region with continued accretion of low-angular momentum material onto the forming cluster core leads to the build-up of a core of massive stars there (Bonnell, Bate & Zinnecker 1998; Klessen 2001), which is tentatively supported by observational data for very young clusters and older open clusters (Raboud & Mermilliod 1998).

The initial distribution functions that are needed to describe a stellar population are the IMF, the period and eccentricity distribution functions. The IMF is conveniently (for computational purposes) taken to be a multi-power-law form,

$$\xi(m) = k \begin{cases} \left(\frac{m}{m_H}\right)^{-\alpha_0} & , \quad m_l < m \leq m_H, \\ \left(\frac{m}{m_H}\right)^{-\alpha_1} & , \quad m_H < m \leq m_0, \\ \left[\left(\frac{m_0}{m_H}\right)^{-\alpha_1}\right] \left(\frac{m}{m_0}\right)^{-\alpha_2} & , \quad m_0 < m \leq m_1, \\ \left[\left(\frac{m_0}{m_H}\right)^{-\alpha_1} \left(\frac{m_1}{m_0}\right)^{-\alpha_2}\right] \left(\frac{m}{m_1}\right)^{-\alpha_3} & , \quad m_1 < m \leq m_2, \\ \left[\left(\frac{m_0}{m_H}\right)^{-\alpha_1} \left(\frac{m_1}{m_0}\right)^{-\alpha_2} \left(\frac{m_2}{m_1}\right)^{-\alpha_3}\right] \left(\frac{m}{m_2}\right)^{-\alpha_4} & , \quad m_2 < m \leq m_u, \end{cases} \quad (1)$$

where  $k$  contains the desired scaling, and  $dN = \xi(m) dm$  is the number of stars in the mass interval  $m$  to  $m + dm$ . Eq. 1 is the general form of a five-part power-law form, but at present observations only support a three-part power-law IMF (Kroupa 2002) with  $m_l = 0.01 M_\odot$ ,  $m_H = 0.08 M_\odot$ ,  $m_0 = 0.5 M_\odot$ , and  $\alpha_2 = \alpha_3 = \alpha_4$ ,

$$\begin{aligned} \alpha_0 &= +0.3 \pm 0.7 & , & \quad 0.01 \leq m/M_\odot < 0.08, \\ \alpha_1 &= +1.3 \pm 0.5 & , & \quad 0.08 \leq m/M_\odot < 0.50, \\ \alpha_2 &= +2.3 \pm 0.3 & , & \quad 0.50 \leq m/M_\odot. \end{aligned} \quad (2)$$

The multi-part power-law form is convenient because it allows an analytic mass-generation function to be used which leads to very efficient generation of masses from an ensemble of random deviates. The multi-part power-law form also has the significant advantage that various parts of the IMF can be changed without affecting other parts, such as changing the number of massive stars by varying  $\alpha_4$  without affecting the form of the luminosity function of low-mass stars. Other functional descriptions of the IMF are in use (e.g. Chabrier 2001).

The initial period distribution function needs to be consistent with the TA data, and a convenient form which also has an analytic period-generation function is derived in K2,

$$f_{P,\text{birth}} = 2.5 \frac{(lP - 1)}{45 + (lP - 1)^2}, \quad (3)$$

where  $f_{P,\text{birth}} d lP$  is the proportion of binaries among all systems with periods in the range  $lP$  to  $lP + dlP$  ( $P$  in days throughout this paper), and  $1 \leq lP \equiv \log_{10} P$ . The usual notation for the binary proportion is used here,  $f_P = N_{\text{bin},P}/N_{\text{sys}}$ , where  $N_{\text{sys}} = N_{\text{bin}} + N_{\text{sing}}$  is the number of systems and  $N_{\text{bin},P}$  is the number of binary systems with periods in the bin  $lP$ . The condition  $\int_{lP} f_{P,\text{birth}} d lP = 1$  (all stars being born in binaries) gives  $P_{\text{max}} = 10^{8.43}$  d for the maximum period obtained from the distribution 3.  $N$ -body experiments demonstrate that the observed range of periods ( $P \approx 10^{0-9}$  d) must be present as a result of the star-formation process; encounters in very dense sub-groups cannot sufficiently widen initially more restricted period distributions and at the same time lead to the observed fraction of binaries in the Galactic field (Kroupa & Burkert 2001). Observations show that the eccentricity distribution of Galactic-field binary systems is approximately thermal,  $f_e = 2e$ , and  $N$ -body calculations demonstrate that such a distribution must be primordial because encounters of young binaries in their embedded clusters cannot thermalize an initially different distribution (K2; Kroupa & Burkert 2001).

Binary systems in the Galactic field with short periods ( $P \lesssim 10^3$  d) do show departures from simple pairing by having a bell-shaped eccentricity distribution and a mass-ratio distribution that appears to deviate from random sampling from the IMF. This is apparent most dramatically in the eccentricity–period diagram which shows an upper eccentricity-envelope for short-period binaries (Duquennoy & Mayor 1991). This indicates that binary-system–internal processes may have evolved a primordial distribution. Such processes are envelope–envelope or disk–disk interactions during youth, shared accretion during youth, rapid tidal circularisation during youth, and slow tidal circularisation during the main-sequence phase. These system-internal processes that change the orbital parameters cannot be expressed with only a few equations given the extremely complex physics involved, but a simple analytical description is available through the K2-formulation of *eigenevolution–feeding*. Feeding allows the mass of the secondary to grow, while eigenevolution allows the eccentricity to circularise and the period to decrease at small peri-astron distances, and merging to occur if the semi-major axis of the orbit is smaller than 10 Solar radii. About 3 per cent of initial binaries merge to form a single star. The eigenevolved model-main-sequence eccentricity–

period diagram, and the eccentricity and mass-ratio distributions of short-period systems, agree well with observational data. In particular, although the minimum period obtained from eq. 3 is  $P = 10$  d, eigenevolution leads to the correct number of  $P < 10$  d periods. The resulting IMF of all stars shows slight departures from the input IMF (eq. 2) as a result of the mass-growth (feeding) of some secondaries, but the deviations are well within the IMF uncertainties.

### 3 MODELS OF TAURUS–AURIGA-LIKE AGGREGATES

A star-formation event produces a spatial distribution of stars which is typically centrally concentrated. As a first approach, this density distribution is assumed to be smooth without sub-structure, because this minimises the number of parameters needed. Each binary system is thus provided with phase-space variables which define its initial location and velocity relative to the other binaries. A mathematically very convenient smooth spatial distribution function is given by the Plummer model,

$$\rho(R) = \frac{3 N_{\text{bin}}}{4 \pi R_{\text{pl}}^3} \frac{1}{[1 + (R/R_{\text{pl}})^2]^{5/2}}, \quad (4)$$

where  $N_{\text{bin}}$  is the number of binary systems in the aggregate or cluster, and  $R_{0.5} = 1.305 R_{\text{pl}}$  is the half-mass radius. For each position the associated velocity needs to satisfy Poisson’s equation; the generating functions for position and velocity variables are presented in Aarseth, Hénon & Wielen (1974).

To study the dynamical evolution of TA-like aggregates 25 binaries are distributed as a Plummer density distribution embedded in an analytical background gas potential with the same  $R_{0.5}$  as the stars, but twice the stellar mass. The star-formation efficiency in the aggregate is thus assumed to be 33 per cent ( $\epsilon = 0.33$ ; Lada 1999). The velocity of each binary-star centre-of-mass is  $v_{\text{bin,g}} = v_{\text{bin}}/\sqrt{\epsilon}$  to insure initial dynamical equilibrium, where  $v_{\text{bin}}$  is the velocity in an equilibrium aggregate without gas. Assuming dynamical equilibrium is equivalent to assuming that the stars form from condensations in a cloud core in virial equilibrium. The gas potential is kept constant for a time  $\tau_{\text{D}}$  after which it begins to evolve on an exponential time-scale  $\tau_{\text{M}}$ . Different values for  $\tau_{\text{D}}$  and  $\tau_{\text{M}}$  test the effect on the binary population of having the aggregates embedded in the potential for time scales ranging from a fraction to about two crossing times. Each model is integrated for 40 Myr, by which time the aggregates have largely dissolved. All stars and binaries are kept in memory for data reduction, for which a separate software package has been written. Briefly, GASEx writes out snapshots of all data at regular time intervals. These are used to find all bound binary systems and single stars and other data relevant for the present discussion. We note that a more self-consistent treatment of gas-expulsion using the smooth-particle-hydrodynamics approximation to model the gas dynamics leads to the same results as when applying a time-varying analytical background potential (Geyer & Burkert 2001).

The models are listed in Table 1. The half-mass radii and number of systems are chosen to reflect the observed values (Gomez et al. 1993; Hartmann, Ballesteros-Paredes & Bergin 2001; Briceno et al. 2002; Palla & Stahler 2002). The durations of the embedded phase ( $\approx t_{\text{D}} + 2\tau_{\text{M}}$ ) approximately span the duration of star formation and is typically longer than the crossing time – the residual gas is removed over time through the accumulating stellar outflows (Matzner & McKee 2000). There are 140 renditions per model with different initial random number seeds. The IMF power-law index in the BD mass range,  $\alpha_0$ , is changed between some of the models to allow an investigation of various BD contents. The table also contains the two KAH models of dense and rich ONC-type clusters. These models are constructed in exactly the same way as the present TA-like models, and thus allow a consistent comparison of the evolution of the binary population and the apparent IMF with empirical data to test for possible deviations from the standard model.

### 4 DYNAMICAL EVOLUTION

An outline of the dynamical evolution and associated changes of the stellar population is given in this section.

The aggregates evolve by expanding due to two-body encounters and the removal of the gas. Snapshots of this are shown in Figs 1 and 2. The density profiles of stellar- and BD-systems are plotted at various times in Figs. 3 (model T0) and 4 (model T5). The dissolution of the aggregates is evident by the reduction with time of the number densities, and the figure also shows that the BD and stellar populations do not separate significantly in these models. That is, the BDs trace the stars, except for a small high-velocity BD distribution which results from BDs being ejected in binary–binary encounters (Figs. 16 and 17 below).

The nominal dissolution time due to redistribution of energy within the aggregates due to two-body encounters is  $t_{\text{diss}} \approx 100 t_{\text{relax}}$ , where  $t_{\text{relax}} \approx 0.1N t_{\text{cross}}/\ln N$  is the median two-body relaxation time (Binney & Tremaine 1987). For models T0–T5  $t_{\text{relax}} \approx 0.8 - 1.3$  Myr for  $N_{\text{sys}} = 25 - 50$ , so that  $t_{\text{diss}} \approx 80 - 130$  Myr. Gas removal unbinds the aggregates on a much shorter time-scale though, as is shown in Figs 5 and 6. Thus, by 32 Myr models T0, T1, T2 and T5 contain on average only about 2, 5, 7 and 7 systems within the central 1 pc sphere, respectively.

The number of BD systems within the central 1 pc sphere increases at first as a result of BD companions being freed from binary systems, but at later times ( $t \gtrsim 5$  Myr) the relative number of BDs decays more rapidly than the number of

**Table 1.** Initial cluster models. For each except models A & B there are 140 realisations with different initial random number seeds.  $N_{\text{sing}}, N_{\text{bin}}$  are the average number of single stars and binaries, respectively (each model shows deviations as a result of initial disruption due to overlapping binaries and binary-star *eigenevolution* during the pre-main sequence phase which can lead to a binary merging to a single star); the average stellar mass is  $\langle m \rangle$  – for models T0 & T1 the range of masses allowed is  $0.01 - 5.0 M_{\odot}$ , while for models T2–T5 it is  $0.01 - 2.0 M_{\odot}$ , and for the KAH models A & B the range is  $0.01 - 50 M_{\odot}$ ;  $\sigma_{3D}$  is the 3D velocity dispersion of systems;  $t_{\text{cross}} = 2 R_{0.5} / \sigma_{3D}$  is the nominal crossing time;  $\rho_C$ : central number density;  $M_{\text{st}}, M_{\text{g}}$ : mass in stars and gas, respectively, these are average values of the 140 renditions per model;  $\tau_M$ : time-scale for gas expulsion (eq. 2 in KAH);  $t_D$ : onset of gas-expulsion; the stellar and gas distributions have half-mass radii  $R_{0.5}, R_{0.5,g} (R_{\text{pl,g}}(0) = 0.766 R_{0.5,g})$ , respectively. The BD population is described by the IMF power-law index  $\alpha_0$ , and the fraction of the population that are BDs is given by the last column.

model	$N_{\text{sing}}$	$N_{\text{bin}}$	$R_{0.5}$	$\langle m \rangle$	$\sigma_{3D}$	$t_{\text{cross}}$	$\log_{10} \rho_C$	$M_{\text{st}}$	$M_{\text{g}}$	$R_{0.5,g}$	$\tau_M$	$t_D$	$\alpha_0$	$N_{\text{BD}}/N_{\text{st}}$
			[pc]	$[M_{\odot}]$	[km/s]	[Myr]	[stars/pc <sup>3</sup> ]	$[M_{\odot}]$	$[M_{\odot}]$	[pc]	[Myr]	[Myr]		[per cent]
T0	2	23	0.30	0.32	0.51	1.2	3.0	16	32	0.30	1.0	0.5	+0.3	37
T1	1	24	0.80	0.32	0.31	5.2	1.7	16	32	0.80	1.0	0.5	+0.3	37
T2	1	24	0.30	0.35	0.53	1.1	3.0	18	36	0.30	2.0	2.0	-4.2	10
T3	1	24	0.30	0.35	0.53	1.1	3.0	18	36	0.30	2.0	2.0	-3.0	12
T4	1	24	0.30	0.33	0.51	1.2	3.0	17	34	0.30	2.0	2.0	-1.5	18
T5	1	24	0.30	0.30	0.49	1.2	3.0	15	30	0.30	2.0	2.0	-0.5	26
A	575	4642	0.450	0.38	6.8	0.13	4.8	3746	7492	0.450	0.045	0.60	+0.3	37
B	1247	4298	0.206	0.42	10.8	0.038	5.8	4170	8340	0.206	0.021	0.60	+0.3	37

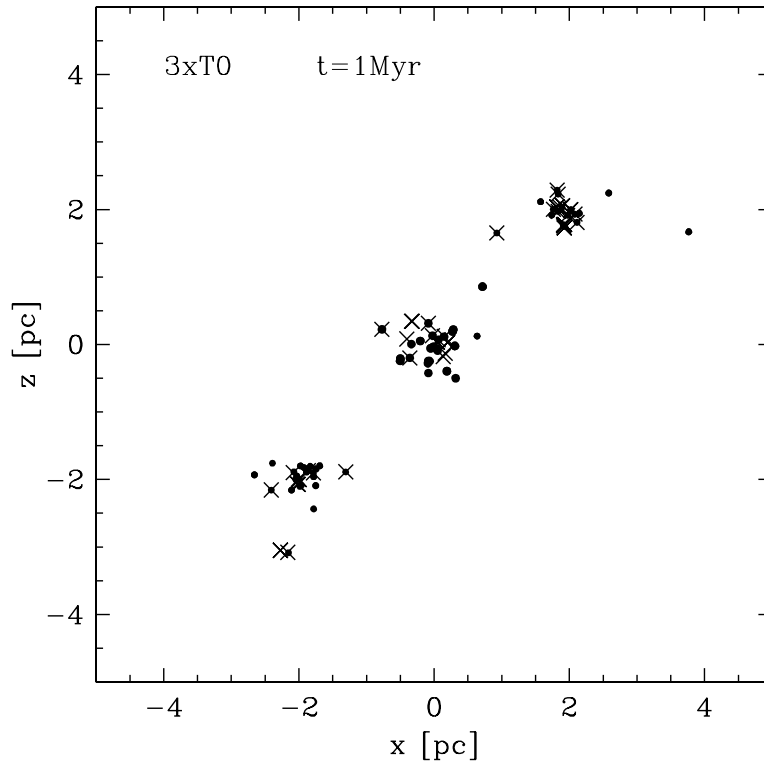


**Figure 1.** The appearance of the first three of the 140 T0 aggregates after 1 Myr. Crosses denote BDs, many of which are in binaries with stellar (dots) primaries. At this age each aggregate contains about  $20 M_{\odot}$  of gas and is thus still embedded, with the fraction of gas mass being slightly larger than the mass in stars and BDs ( $16 M_{\odot}$ ). The relative motion of the aggregates is neglected. The  $z$ -direction is perpendicular to the Galactic plane, while the  $x$ -direction is arbitrary within the Galactic plane.

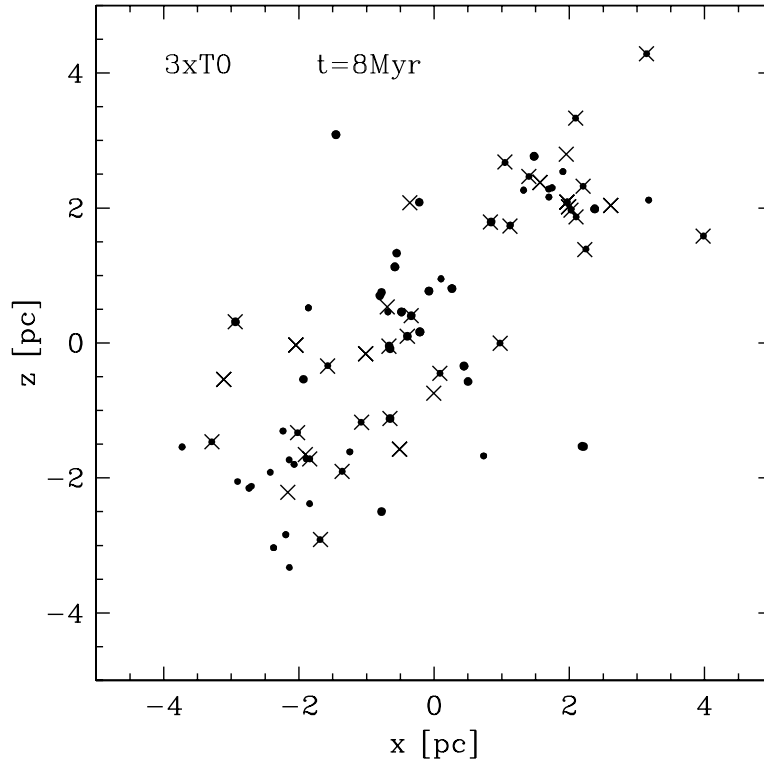


**Figure 2.** As fig. 1 but at 8 Myr.

stellar systems as a result of energy equipartition in the aggregates and gas removal (Fig. 7). During the embedded phase the BDs acquire on average somewhat higher velocities than the stars leading to their slightly more rapid dispersal after the gas has been removed (§ 6). The net effect is nevertheless such that at 0, 1 and about 15 Myr the BD- and stellar-systems have statistically indistinguishable density profiles (Figs 3 and 4).

The core radius (eq. 11 in KAH), which indicates that radius by which the luminosity density has fallen to half its central value, is shown in Fig. 8. It expands substantially and becomes larger than 1 pc by 6–8 Myrs for models T0 and T1. The slowed expansion due to delayed gas-expulsion in models T2–T5 is evident in Fig. 9, these models retain a more compact morphology and the core radius reaches 1 pc by about 20 Myr.

The evolution of the three-dimensional velocity dispersion within the central 1 pc sphere is shown in Figs. 10 and 11. It drops from an initial 0.6 km/s (models T0, T2–T5) or 0.4 km/s (model T1) to values close to 0.3 km/s or less. These values are consistent with the low stellar velocity dispersion of 0.2 km/s (one dimensional) suggested within the TA cloud filaments by Hartmann (2002).

The mean system mass within the central 1 pc region indicates the level to which mass segregation develops. It increases only by a small amount in all models (Figs. 12, 13). By about 32 Myr models T0 and T2–T5 have a mean system mass of  $0.39 - 0.45 M_{\odot}$ , while the initially least concentrated model T1 (which has the same IMF as T0) has  $\langle m \rangle \approx 0.25 M_{\odot}$ . Thus, initially more compact aggregates produce final long-lived small- $N$  groups with more massive components, which is a result of the larger probability of partner exchanges in the denser environment.

## 5 THE BINARY SYSTEMS

The binary-star population evolves through system-internal processes (eigenevolution, § 2). This affects only the short-period binaries ( $P \lesssim 10^3$  d). Encounters between binaries disrupt long-period binaries on the crossing time-scale of the aggregate. Binary-system disruption extends approximately down to a characteristic (or “thermal”) period,  $P_{\text{th}}$  [d], at which the circular orbital velocity,  $v_{\text{orb}}$  [km/s], of a binary system with mass  $m_{\text{sys}}$  [ $M_{\odot}$ ], equals the velocity dispersion,  $\sigma_{3\text{D}}$  [km/s], in the cluster.

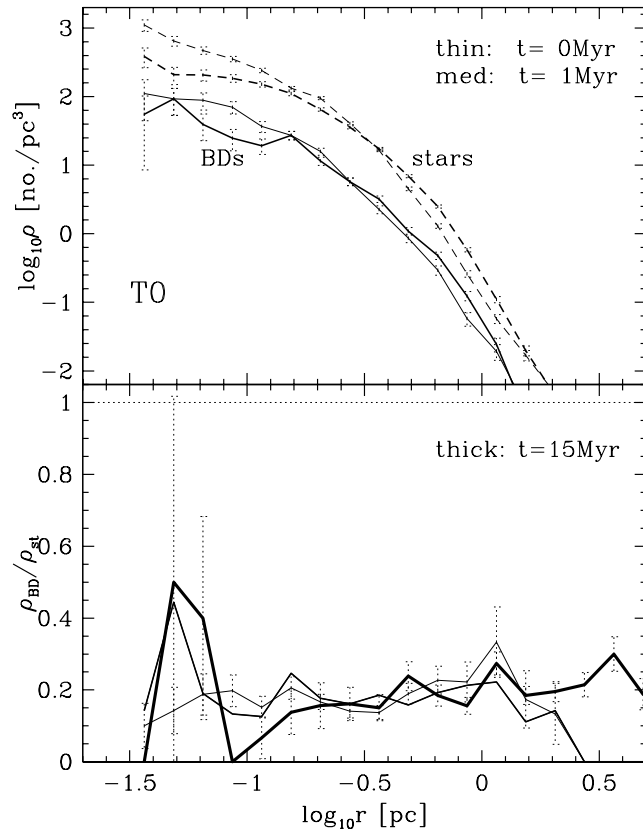


**Figure 3. Upper panel:** The radial density profile of stellar ( $0.08 \leq m_p/M_\odot \leq 1.0$ , dashed lines) and BD systems ( $0.01 \leq m_p/M_\odot \leq 0.08$ , solid lines). A system consists either of a single star or BD or a binary with a stellar or BD primary mass. **Lower panel:** The ratio of the density of stellar- and BD-systems. In both panels the curves are averages of 140 different random-number renditions of model T0.

Because  $\sigma_{3D}$  decreases as the aggregate expands,  $P_{th}$  moves to longer periods until it extends beyond the cutoff period of the evolving period distribution function, which is moving towards  $P_{th}$  (Kroupa 2000). There is not a sharp truncation of the period distribution function however — binaries with  $P > P_{th}$  located in the outer region of the cluster at  $t = 0$  may arrive in the inner parts of the cluster when  $P < P_{th}$  making them resistant against disruption. When the crossover of  $P_{th}$  and  $P_{cut}$  happens, further binary-disruption is mostly halted, and only rare close encounters in the surviving stellar group lead to further changes in the orbital parameters of a few binaries. With

$$\log_{10} P = 6.986 + \log_{10} m_{sys} - 3 \log_{10} v_{orb}, \quad (5)$$

$P = P_{th}$  if  $v_{orb} = \sigma_{3D}$ . For  $\sigma_{3D} = 0.6$  km/s and  $m_{sys} = 0.4 M_\odot$  (Table 1)  $P_{th} = 10^{7.3}$  d, which means that a large number of binaries with periods  $7.3 \lesssim \log P \lesssim 8.3$  will be disrupted implying reduction of  $f_P$  by about 20 per cent. The final binary-fraction should thus be  $f \approx 0.8$ . This is confirmed by the data plotted in Figs. 14 and 15, which also confirm that prior dynamical evolution of the present-day TA groups did not lead to significant changes of the binary-star population. The figures show that BDs retain a significantly smaller binary proportion than stellar primaries. This is a result of the weaker binding energy of BD–BD binaries. Fig. 15 also shows that models T2 and T5 have a significantly smaller BD binary proportion than models T0 and T1. This comes about because models T2–T5 enjoy a longer embedded phase leading to more encounters per system. An effect also playing a role is that T2–T5 have relatively fewer BDs by virtue of the steeply declining IMF for  $m < 0.08 M_\odot$ . A larger fraction of stars is thus obtained implying a larger average mass of the siblings that a typical BD binary encounters, and thus larger relative perturbative forces which are more efficient in destroying the BD binaries than in models T0 and T1.

The evolution of the binary proportion of the ONC-like models of KAH is also plotted in Fig. 14. From Table 1,  $\sigma_{3D} = 6.8$  (model A) and 10.8 (model B), implying  $P_{th} = 10^{4.1}$  d (model A) and  $10^{3.5}$  d. Thus, in ONC-like clusters the period distribution function is cut-off at a much shorter period than in TA-like aggregates despite the same initial period distribution.

To summarize, the important result here is that TA-like aggregates could not have provided significantly to the Galactic-field population which has a binary proportion of about  $f = 0.55 - 0.6$  (Duquennoy & Mayor 1991).

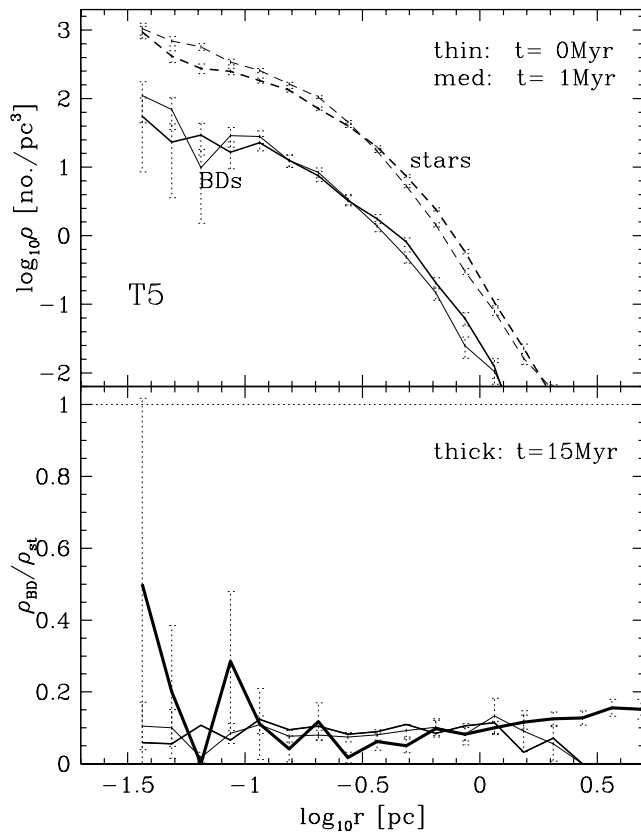


Figure 4. As Fig. 3 but for model T5.

## 6 THE RELATIVE DISTRIBUTION OF BROWN DWARFS AND STARS

The relative distribution of stars and BDs is a potential discriminant between different formation scenarios. For example, the *embryo-ejection hypothesis* according to which BDs are ejected unfinished stars from forming multiple systems (Reipurth 2000; Boss 2001; Reipurth & Clarke 2001; Bate, Bonnell & Bromm 2002) implies a spatially wide distribution of BDs if their typical ejection velocities are about 1 km/s or larger.

In contrast, the standard reference star-formation model (§ 2), which is extended here and in KAH to include BDs, assumes that stars and BDs form with the same kinematical and binary properties at the point when the system can be treated as an  $N$ -body system. For TA-like aggregates the standard model with BDs implies that the BDs and stars trace approximately the same density distribution (Figs. 3 and 4). Close encounters between binaries eject, from the temporary four and later three-body system, preferentially the least massive members, i.e. typically the BDs (Sterzik & Durisen 1998). The standard model should thus yield, for the BDs, a high-velocity tail populated almost exclusively by single BDs. This is evident in Figs. 3 and 4 by the slightly increasing ratio  $\rho_{\text{BD}}/\rho_{\text{st}}$  with increasing  $r$  at late times. The ejected BDs will also have truncated disks with a truncation radius of about the peri-astron distance that produced the BD escaper. Thus, for an ejection velocity  $\geq 1$  km/s the truncation radius will be  $\leq 40$  AU (eq. 5 plus Kepler’s third law).

This is basically the same result as for the embryo-ejection scenario (Reipurth 2000) which was recently championed by Reipurth & Clarke (2001), making a distinction between both (standard model vs the ejection hypothesis for the origin of BDs) rather difficult if the evidence is based only on a distributed, binary-deficient BD population which also has truncated disks when young. It is thus essential to use the entire information, namely the binary properties in dependence of the locations and velocities of the BD population. Thus, the embryo-ejection hypothesis implies a shallow density distribution of mostly single BDs extending to large distances, while the standard model implies a density distribution which is similar to that of the stars with an extended low-density tail of mostly single BDs. The fraction of BDs per star as a function of distance from the aggregate centre (Figs 3, 4) is thus an observational diagnostic that should help distinguishing the two models.

The velocity distribution functions are quantified in Figs. 16 and 17 for models T0 and T5, respectively (the other models T2–T4 yield very similar results, while model T1 has a narrower velocity distribution and a much smaller ejection tail).

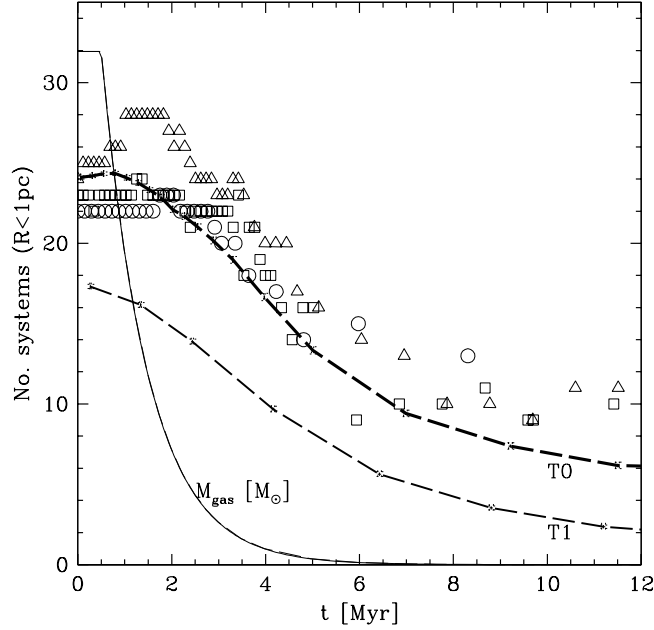


**Figure 5.** The number of systems (all masses) located within 1 pc of the density centre of the ensemble of TA-like aggregates is shown as the dashed lines. The thick curve denotes the average of 140 T0 models, while the thin curve is the average of 140 T1 models. Errorbars are standard deviation of the mean values. Open triangles, squares and circles are the three T0 models shown in Figs. 1 and 2. The gas mass of one of the models T0 is shown as the thin solid curve.

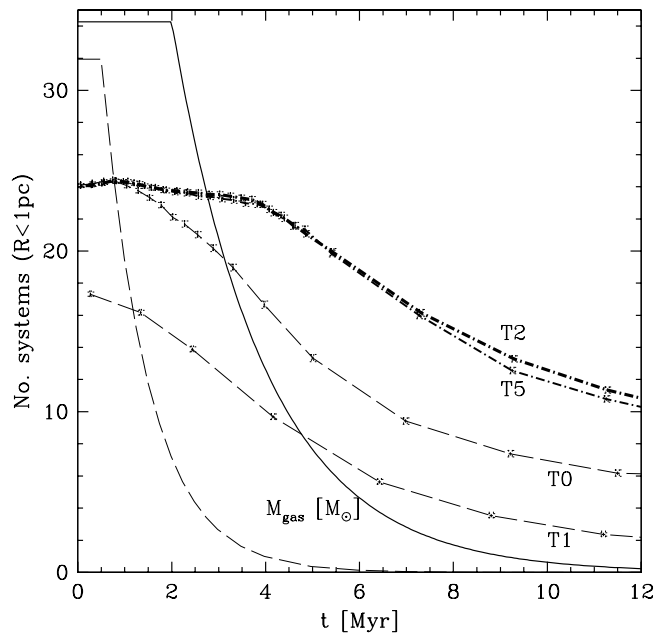


**Figure 6.** As Fig. 5 but showing models T2 and T5 in comparison with models T0 and T1. Note the longer embedded phase and the resulting longer life-time of T2 and T5. The gas mass of one of the 140 T2 models is shown as the solid curve and is initially  $34 M_{\odot}$ , while the dashed curve is  $M_{\text{gas}}(t)$  for one of the T0 models.

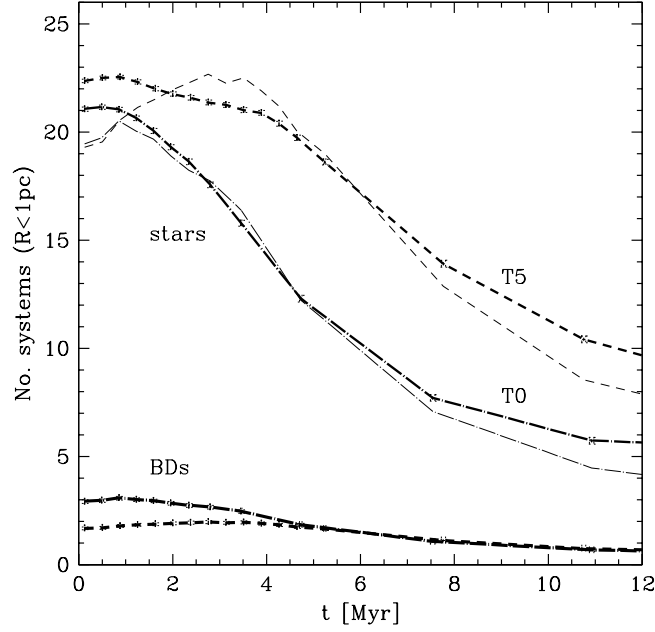


**Figure 7.** The number of BD systems (primaries with masses  $0.02 - 0.08 M_{\odot}$ ) within a distance of 1 pc of the aggregate centres in models T0 and T5 are plotted as the thick curves (dot-dashed: T0; dashed: T5). They are (arbitrarily) scaled to become the corresponding thin curves to show the evolution relative to the number of stellar systems (primaries with masses  $0.08 - 10 M_{\odot}$ ) depicted as the upper thick curves.

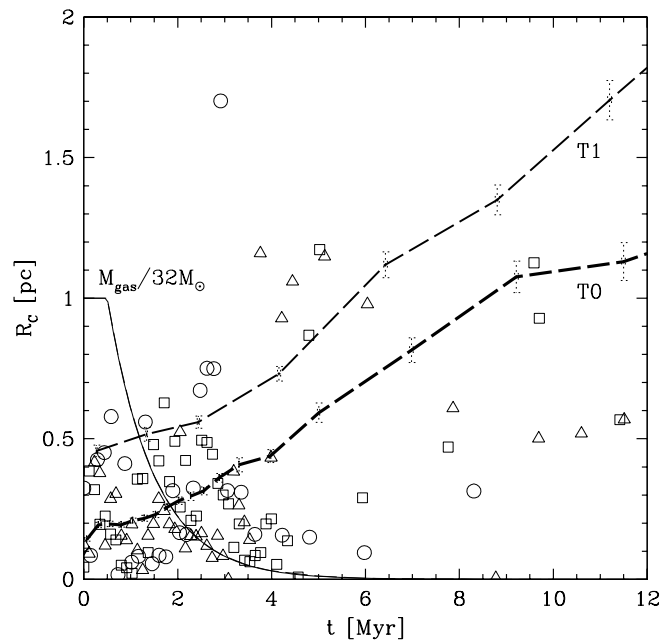


**Figure 8.** The evolution of the core radius. The thick dashed curve shows the average of 140 T0 models, while the thin dashed curve is the average of 140 T1 models. Errorbars are standard deviation of the mean values. Open triangles, squares and circles are the three T0 models shown in Figs. 1 and 2. The gas mass of one of the models T0 is shown as the thin solid curve.

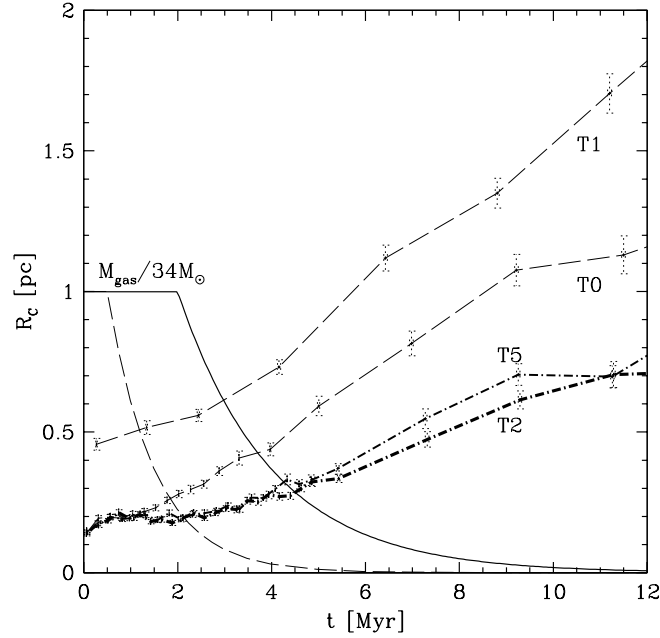


**Figure 9.** As Fig. 8 but showing models T2 and T5 in comparison with models T0 and T1. The gas mass of one of the 140 T2 models is shown as the solid curve and is initially  $34 M_{\odot}$ , while the dashed curve plots  $M_{\text{gas}}(t)$  for one of the T0 models.

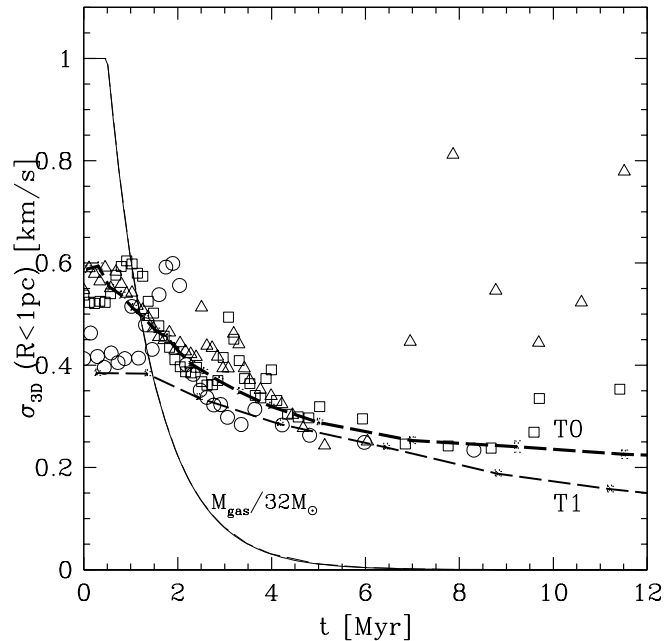


**Figure 10.** The three-dimensional velocity dispersion of systems located within 1 pc of the density centre of each TA-like aggregate is shown as the dashed lines. The thick curve denotes the average of 140 T0 models, while the thin curve is the average of 140 T1 models. Errorbars are standard deviation of the mean values. Open triangles, squares and circles are the three T0 models shown in Figs. 1 and 2. The gas mass of one of the models T0 is shown as the thin solid curve.

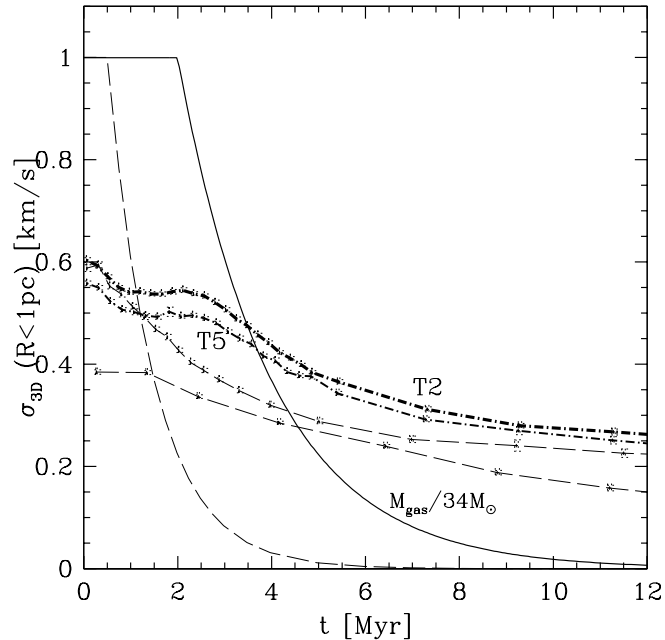


**Figure 11.** As Fig. 10 but showing models T2 and T5 in comparison with models T0 and T1. Note the longer embedded phase and the resulting larger velocity dispersion of T2 and T5. The gas mass of one of the 140 T2 models is plotted as the solid curve, while the dashed curve depicts the gas mass for one of the T0 models.

Model T5 enjoys a longer embedded phase which leads to a more pronounced high-velocity tail for BDs, since the system remains in a more compact configuration for a longer time allowing more encounters than in model T0.

By about 15 Myr about 15 per cent of all BD systems have a velocity larger than 1 km/s in both models. The final stellar velocity distribution is centred on smaller velocities in T5 than in model T0. This results from the slower gas-removal allowing the stellar orbits to adjust more to the changing conditions than in model T0 (T5 is more adiabatic than T0), while the BD population has more time to be accelerated to higher velocities on average by the encounters with the stellar members. Effectively, models T5 (and T2–T4) thus lead to a more pronounced kinematical separation between stars and BDs. This effect will, however, be difficult to observe for any individual aggregate because of the small number of systems per aggregate (see Figs. 1 and 2).

The figures also show the binary proportion as a function of velocity. The ejected BDs have a low if not negligible binary proportion (as for the embryo-ejection hypothesis), and their binary proportion is systematically smaller in the velocity interval 0.4–1 km/s than that of stellar primaries. The standard model with BDs implies that the BDs retain a high binary proportion for  $v \lesssim 0.6$  km/s. Such BDs are spatially distributed similarly to the stars. This last point is an important observable diagnostic distinguishing the embryo-ejection hypothesis from the standard model with BDs, given that the likelihood for ejection of two embryos that become a binary BD is exceedingly small.

## 7 CONCLUDING REMARKS

The dynamical evolution of Taurus–Auriga-like populations is studied using high-precision  $N$ -body computations of embedded aggregates of 25 binaries with different initial concentrations. The aggregates remove their gas on time-scales of a fraction to a few crossing times. The standard model (random pairing from the IMF, no correlation between binary-star orbital parameters and primary mass, and no initial mass segregation) is used to define the input population.

The aggregates disperse within about 10 Myr leaving a population that is dynamically largely unevolved. In particular, the binary population remains high with  $f > 0.8$ . This shows that for the initial conditions chosen for the aggregates, the binary destruction by  $N$ -body processes is minor and leaves a population that is rich in binaries as that observed. Taurus–Auriga-type star formation can therefore be only a minor contributor to the Galactic field population which has  $f = 0.55–0.6$ .

The distributed BD population has a negligible binary proportion and truncated disks, as a result of this population component being preferably ejected during binary–binary encounters from the aggregates. This makes it difficult to empirically

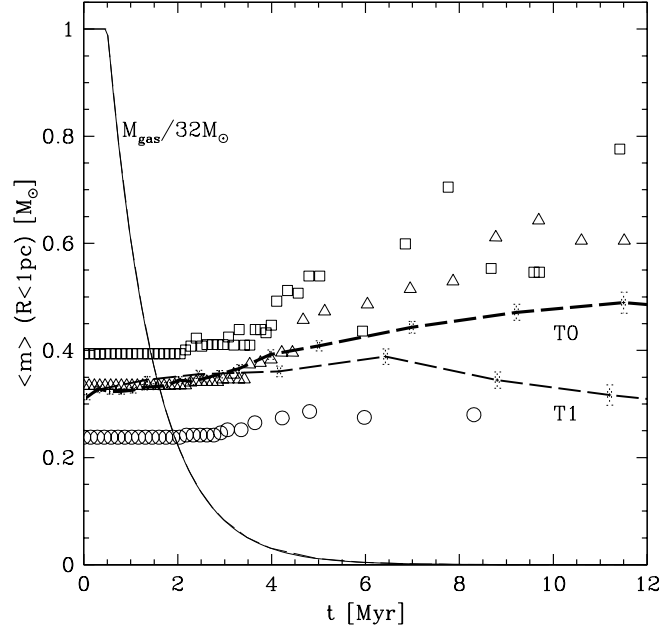


**Figure 12.** The mean mass of systems located within 1 pc of the density centre of each TA-like aggregate is shown as the dashed lines. Thick curves denote the average of the 140 T0 models, while the thin curve is the average of 140 T1 models. Errorbars are standard deviation of the mean values. Open triangles, squares and circles are the three T0 models shown in Figs. 1 and 2. Note the difference in the initial values which stem from statistical variations and feeding. The gas mass of one of the models T0 is shown as the thin solid curve.

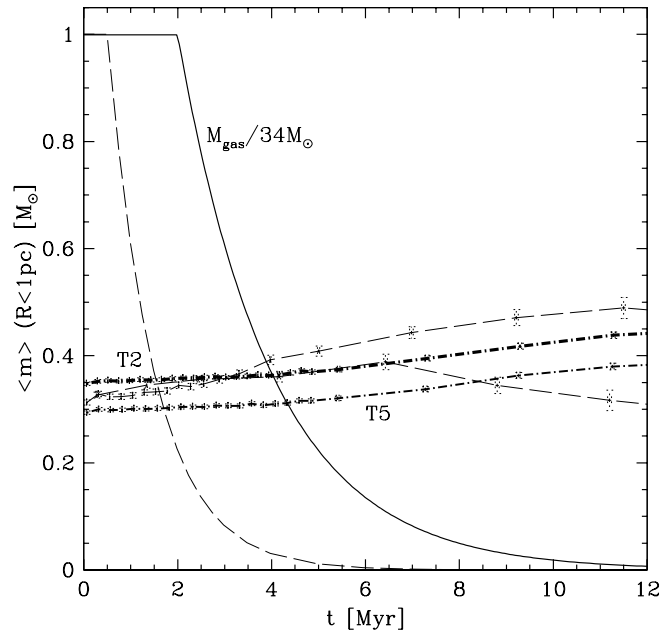


**Figure 13.** As Fig. 12: models T2 and T5 in comparison with models T0 and T1. The gas mass of one of the 140 T2 models is depicted as the solid curve and is initially  $34M_{\odot}$ . The dashed curve is the gas mass for one of the T0 models.

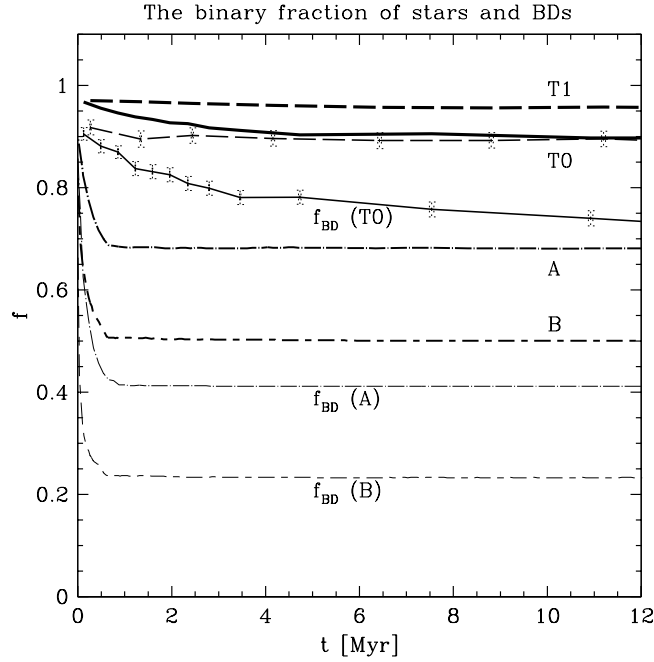


**Figure 14.** The evolution of the binary fraction for models T0 and T1. Thick curves are the binary fraction of stellar primaries ( $0.15 \leq m_1/M_\odot \leq 1.0$ ), while thin curves are the binary fraction of BD primaries,  $f_{BD}$  ( $0.02 \leq m_1/M_\odot \leq 0.08$ ). The curves are averages of 140 renditions of each model, and the errorbars are standard deviations of the mean. For comparison, the evolution of the corresponding quantities in rich ONC-like clusters is indicated by models A and B from KAH.

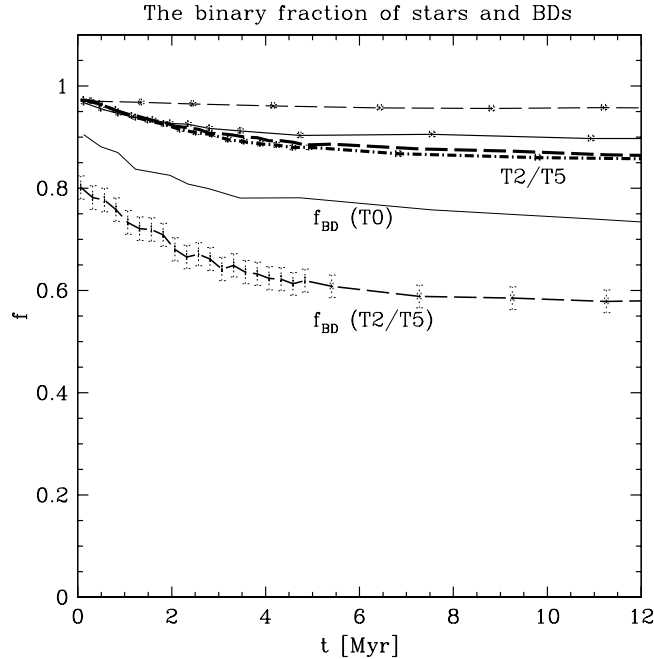


**Figure 15.** As Fig. 14 but showing models T2 and T5 in comparison with models T0 and T1 ( $f_{BD}(T1)$  is not plotted for clarity).

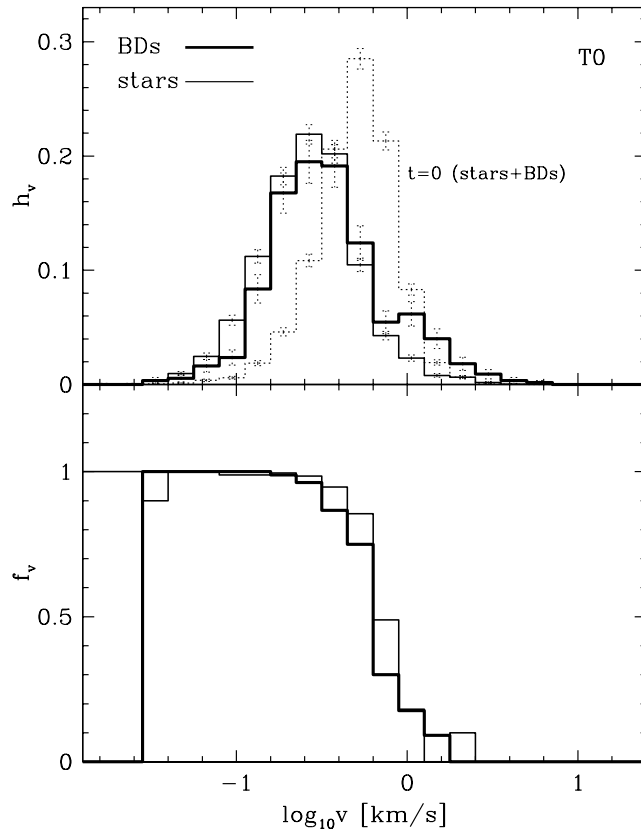


**Figure 16. Upper panel:** The average initial velocity distribution of all stellar and BD systems in model T0 is shown by the thin dotted histogram. At late times ( $t > 10$  Myr) the BD and stellar distributions have separated. The systems with stellar primaries (thin solid histogram) still approximately follow a log-normal distribution but with a reduced mean  $\log_{10}v$  due to gas removal and expansion of the aggregate. The BDs (thick solid histogram) have an appreciable high-velocity ( $\log_{10}v > 1$  km/s) tail which results from the ejections due to binary–binary encounters. The velocity distribution functions are normalised to unit area. **Lower panel:** The thin solid histogram is the velocity-dependent binary proportion,  $f_v$ , of stellar primaries. The thick solid histogram is  $f_v$  of BD primaries. In both panels averages of 140 model renditions are plotted, and the errorbars are standard deviation of the mean values.

verify the hypothesis that BDs may originate as ejected unfinished stellar embryos from few-body systems using the binary proportion, disk truncation and wide spatial distribution of BDs as sole evidence. However, according to the standard model used here (i.e. BDs form with the same kinematical, spatial and binary properties as stars), slow BDs which also share a similar spatial distribution as the stars retain a high binary proportion. This is a powerful distinguishing diagnostic from the embryo-ejection hypothesis, because the slow-moving population is much easier to find given that it overlaps the stellar distribution.

The computations presented here focus on T-A aggregates, but are equally applicable to other young low-mass populations. For example, Chauvin et al. (2002) find the  $\lesssim 5$  Myr old MBM12 association to have an excess binary fraction over Galactic field G and M dwarfs. This may be explainable through an origin of the MBM12 stars in low-mass aggregates similar to T-A.

## ACKNOWLEDGEMENTS

We thank Gaspard Duchêne and Estelle Moraux for useful discussions. PK thanks the staff of the Observatoire de Grenoble for their very kind hospitality and the Université Joseph Fourier for supporting a very enjoyable and productive stay during the summer of 2002.

## REFERENCES

- Aarseth S.J., Hénon M., Wielen R., 1974, *A&A*, 37, 183  
 Bate M.R., 2003, in *IAU Symp.* 211, Martin E.L. et al. (eds.), in press

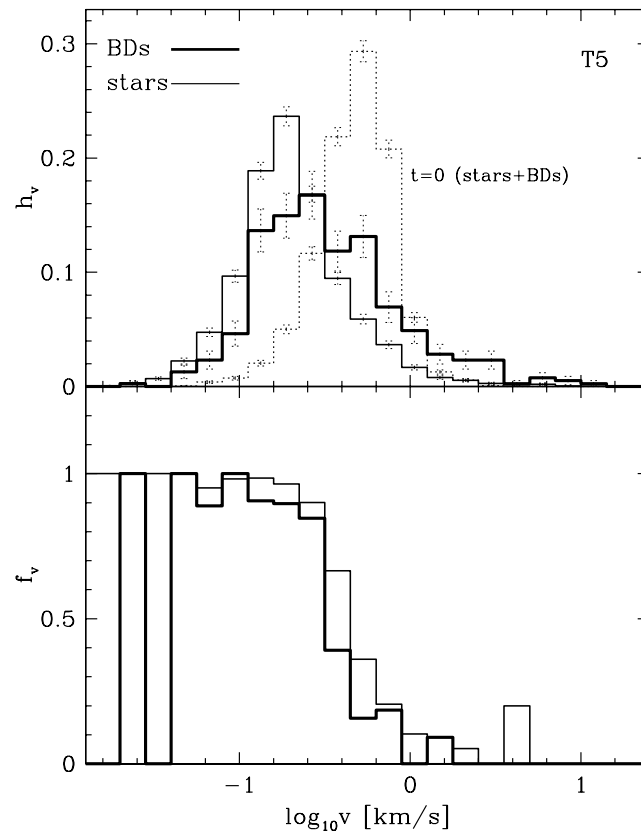


Figure 17. As Fig. 16 but showing model T5.

Bate M.R., Bonnell I.A., Bromm V., 2002, MNRAS, 332, L65  
 Binney J., Tremaine S., 1987, Galactic Dynamics, Princeton University Press, Princeton  
 Bonnell I.A., Davies M.B., 1998, MNRAS, 295, 691  
 Bonnell I.A., Bate M.R., Zinnecker H., 1998, MNRAS, 298, 93  
 Bontemps S., Andr P.; Kaas A.A., et al., 2001, A&A, 372, 173  
 Boss A.P., 2001, ApJ, 551, L167  
 Briceño C., Luhman K.L., Hartmann L., Stauffer J.R., Kirkpatrick J.D., 2002, ApJ, 580, 317  
 Cesaroni R., Codella C., Furuya R.S., Testi L., 2003, A&A, in press  
 Chabrier G., 2001, ApJ, 554, 1274  
 Chauvin G.; Ménard F.; Fusco T., Lagrange A.-M., Beuzit J.-L., Mouillet D., Augereau J.-C., 2002, A&A, 394, 949  
 Clarke C.J., Bouvier J., 2000, MNRAS, 319, 457  
 Duchêne G., 1999, A&A, 341, 547  
 Duquennoy A., Mayor M., 1991, A&A, 248, 485  
 Figueredo E., Blum R.D., Damiani A., Conti P.S., 2002, AJ, in press (astro-ph/0204348)  
 Geyer M.P., Burkert A., 2001, MNRAS 323, 988  
 Gomez M., Hartmann L., Kenyon S.J., Hewett R., 1993, AJ, 105, 1927  
 Hartmann L., 2002, ApJ, 578, 914  
 Hartmann L., Ballesteros-Paredes J., Bergin E.A., 2001, ApJ, 562, 852  
 Hillenbrand L.A., 1997, AJ, 113, 1733  
 Hillenbrand L.A., Hartmann L.W., 1998, ApJ, 321, 540  
 Hillenbrand L.A., Carpenter J.M., 2000, ApJ, 540, 236  
 Klessen R.S., 2001, ApJ., 550, L77  
 Kroupa P., 1995, MNRAS, 277, 1507 (K2)  
 Kroupa P., 2000, in Massive Stellar Clusters, C.M. Boily, A. Lancon (eds), ASP Conf. Ser. 211, 233  
 Kroupa P., 2001, MNRAS, 322, 231  
 Kroupa P., 2002, Science, 295, 82 (astro-ph/0201098)  
 Kroupa P., Bouvier J., 2003, MNRAS, in prep.  
 Kroupa P., Burkert A., 2001, ApJ, 555, 945  
 Kroupa P., Aarseth S.J., Hurley J., 2001, MNRAS, 321, 699 (KAH)  
 Kroupa P., Bouvier J., Duchêne G., Moraux E., 2003, MNRAS, submitted

- Kroupa P., Petr M.G., McCaughrean M.J., 1999, *NewA*, 4, 495
- Lada E.A., 1999, in *NATO Science Series C Vol. 450, The Origins of Stars and Planetary Systems*, ed. C.J. Lada & N.D. Kylafis (Dordrecht: Kluwer), 441
- Malkov O., Zinnecker H., 2001, *MNRAS*, 321, 149
- Matzner C.D., McKee C.F., 2000, *ApJ*, 545, 364
- Motte F., André P., Néri R., 1998, *A&A*, 336, 150
- Motte F., Schilke P., Lis D.C., 2002, *ApJ*, in press (astro-ph/0208519)
- Muench A.A., Lada E.A., Lada C.J., Alves J., 2002, *ApJ*, 573, 366
- Muench A.A., Lada E.A., Lada C.J., Elston R.J., Alves J.F., 2003, *AJ*, in press (astro-ph/0301276)
- Palla F., Stahler S.W., 2002, *ApJ*, submitted (astro-ph/0208554)
- Raboud D., Mermilliod J.-C., 1998, *A&A*, 333, 897
- Reipurth B., 2000, *AJ*, 120, 3177
- Reipurth B., Clarke C., 2001, *AJ*, 122, 432
- Scally A., Clarke C.J., 2002, *MNRAS*, 334, 156
- Sterzik M.F., Durisen R.H., 1998, *A&A*, 339, 95
- Woitak J., Leinert C., Köhler R., 2001, *A&A*, 376, 982